Electronic Supplementary Material (ESI) for ChemComm.

Supporting Information

DNA–Ligand Interactions Gained and Lost: Light-induced Ligand Redistribution in a Supramolecular Cascade

Daria V. Berdnikova,*[a,b] Tseimur M. Aliyeu,[b] Thomas Paululat,[a] Yuri V. Fedorov,[b] Olga A. Fedorova,[b] and Heiko Ihmels[a]

[a] Department Chemie–Biologie, Organische Chemie II, Universität Siegen, Adolf-Reichwein-Str. 2, 57068 Siegen, Germany

[b] A. N. Nesmeyanov Institute of Organoelement Compounds, Russian Academy of Sciences, Vavilova str. 28, 119991 Moscow, Russia

berdnikova@chemie-bio.uni-siegen.de; daria@ineos.ac.ru

Table of Contents:

1. Materials and Methods

All reagents and solvents were obtained from commercial sources and used as received. (2-Hydroxypropyl)-*β*-cyclodextrin with average M_w ~1,460 (0.8 molar substitution) was purchased from Sigma Aldrich. Purified water with resistivity ≥ 18 MΩ cm^{-1} was used for preparation of buffer solutions and spectrometric measurements. Na-phosphate buffer (10 mM, pH 7.0) was used for all measurements.

NMR spectra were recorded on a Varian VNMR-S 600 spectrometer equipped with 3 and 5 mm dual broadband and 3mm triple resonance inverse probes. Solvent signals were used as internal standard (Acetone-d6: δ_H = 2.05, δ_C = 29.8 ppm; CD_3CN: δ_H = 1.93, δ_C = 1.28 ppm), all spectra are recorded at T = 25°C. Pulse sequences were taken from Varian pulse sequence library. Spectra in H2O/D2O 9:1 were recorded at T = 25 °C with water suppression using wet sequence.

High-resolution mass spectra were recorded on a time-of-flight mass-spectrometer Bruker MicrOTOF in a positive-ion mode using electrospray ionization method.

Mass spectra (ESI in the positive-ion mode) were recorded with a Finnigan LCQ Deca instrument; only *m*/*z* values in the range of 100–2000 units were analyzed.

Electronic absorption spectra were recorded using a Varian Cary 100 Bio spectrophotometer. Fluorescence spectra were recorded on a Varian Cary Eclipse spectrofluorometer. Circular dichroism spectra were measured with an Applied Photophysics Chirascan CD spectrometer. Spectrophotometric measurements were performed in thermostated quartz sample cells of 10 mm pathlength at 20 ± 1 °C. Preparation and handling of the solutions were carried out under red light. The actual concentrations of DNA samples were determined photometrically using the extinction coefficient ε_{260} = 12824 cm^{-1} M^{-1} (bp). Photochemical reactions were carried out with a high pressure Hg vapor lamp (145 W) and an immersed Hg photoreactor (125 W).

2. Synthesis

Cucurbit[7]uril (purity >95%) was obtained according to the published protocol,[1] and its purity was confirmed by NMR and ESI MS data.

(E)-2-(3,4-dimethoxystyryl)pyridine ***(1)***

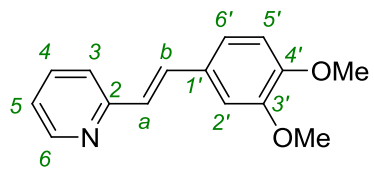

1,2-Dimethylpyridinium iodide (500 mg, 2.13 mmol) and 3,4-dimethoxybenzaldehyde (354 mg, 2.13 mmol) were dissolved in *n*-BuOH (4 mL) with addition of pyrrolidine (0.3 mL). The mixture was stirred at 120 °C under argon during 2 h. Then the solvent was removed in vacuum, the residue was treated with hot benzene. The precipitate was filtered, washed with diethyl ether and dried to give 1-methyl-2-(3,4-dimethoxystyryl)pyridinium iodide (644 mg, 1.70 mmol, yield 85%).

The 1-methyl-2-(3,4-dimethoxystyryl)pyridinium iodide (100 mg, 0.26 mmol) was dissolved in *N*,*N*-dimethylaniline (2 mL) and the solution was stirred at 170 °C under argon during 2.5 h. Then *N*,*N*-dimethylaniline was removed in vacuum, the residue was treated with hot benzene (30 mL), undissolved precipitate was filtered off. The filtrate was evaporated; the remaining residue was purified by column chromatography (Al_2O_3, benzene-ethylacetate going from 1:0 to 100:1) followed by recrystallization from heptane to give the desired product **1** in 77% yield (49.0 mg, 0.20 mmol). ^{1}H NMR (acetone-d_6, 600 MHz) δ: 3.84 (s, 3H, OCH_3), 3.89 (s, 3H, OCH_3), 6.97 (d, J = 8.3, 1H, H-5'), 7.14-7.20 (m, 3H, H-a, H-6', H-5), 7.31 (broad. s, 1H, H-2'), 7.45 (d, J = 7.9, 1H, H-3), 7.67 (d, J_{trans} = 16.1, 1H, H-b), 7.72 (m, 1H, H-4), 8.55 (d, J = 4.8, 1H, H-6). ^{13}C NMR (acetone-d_6, 150 MHz) δ: 55.2 (2C, OCH_3), 109.8 (C-2'), 111.8 (C-5'), 120.8 (C-6'), 121.7 (C-3), 121.8 (C-5), 126.0 (C-a), 129.9 (C-1'), 132.4 (C-b), 136.4 (C-4), 149.5 (C-4'), 149.7 (C-6), 150.1 (C-3'), 156.0 (C-2). Anal. calcd. for $C_{15}H_{15}NO_2$: C, 74.67; H, 6.27; N, 5.81; found: C, 74.61; H, 6.26; N, 5.79.

8,9-(dimethoxy)[3,4]benzo[c]quinolizinium perchlorate ***(2)***

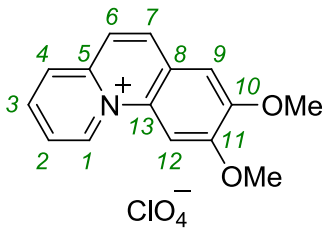

The acetonitrile solution (1.00 mM) of **1** (50.0 mg; 0.21 mmol) was irradiated with an immersed Hg photoreactor (125 W) under UV-Vis spectroscopy control. As soon as maximum conversion was reached the solvent was removed in vacuum, the residue was washed with hexane and recrystallized from MeOH with addition of $HClO_4$ to give the photocyclization product **2** as a perchlorate salt in 57% yield (41.0 mg, 0.12 mmol). ^{1}H NMR (CD_3CN, 600 MHz) δ: 4.06 (s, 3H, OCH_3), 4.20 (s, 3H, OCH_3), 7.67 (s, 1H, H-9), 8.04-8.07 (m, 2H, H-2, H-7), 8.16 (s, 1H, H-12), 8.34 (t, J = 7.3, J = 8.2, 1H, H-3), 8.41 (d, J = 8.2, 1H, H-4), 8.48 (d, J = 8.7, 1H, H-6), 10.01 (d, J = 6.9, 1H, H-1). ^{13}C NMR (CD_3CN, 150 MHz) δ: 56.3 (OCH_3), 57.1 (OCH_3), 99.1 (C-12), 109.0 (C-9), 120.6 (C-10), 122.9 (C-2), 123.5 (C-7), 128.4 (C-4), 130.3 (C-11), 133.1 (C-1), 136.1 (C-6), 137.3 (C-3), 142.5 (C-5), 152.0 (C-8), 154.8 (C-13). Anal. calcd. for $C_{15}H_{14}ClNO_6$: C, 53.03; H, 4.15; N, 4.12; found: C, 53.05; H, 4.18; N, 4.11. HRMS *m/z* 240.1028 [**2**]$^+$ (calcd. for $C_{15}H_{14}NO_2$, 240.1019).

3. Supramolecular Interactions

*3.1. Styrylpyridine derivative **1** – HP-β-CD interaction*

Absorption, fluorescence and circular dichroism spectroscopy

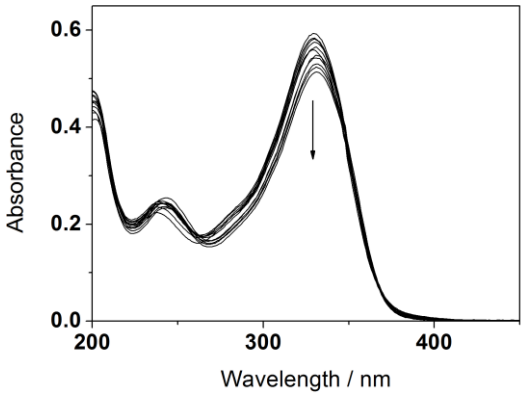

Figure S1. Spectrophotometric titration of HP-*β*-CD to **1** ($c_{\mathbf{1}}$ = 20 μM, $c_{\text{HP-}\beta\text{-CD}}/c_{\mathbf{1}}$ = 0–1000) in phosphate buffer (pH 7.0) at 20 °C.

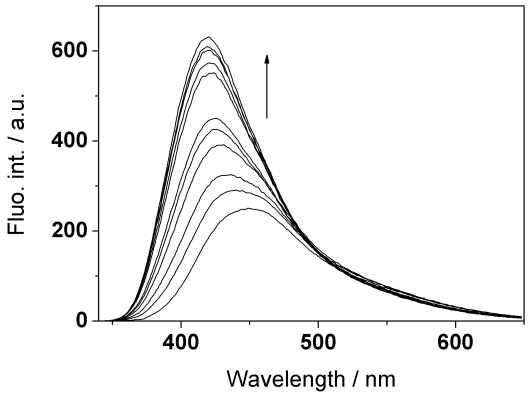

Figure S2. Fluorimetric titration of HP-*β*-CD to **1** (λ_{ex} = 330 nm, c = 20 μM, $c_{\text{HP-β-CD}}/c_{\mathbf{1}}$ = 0–1000) in phosphate buffer (pH 7.0) at 20 °C.

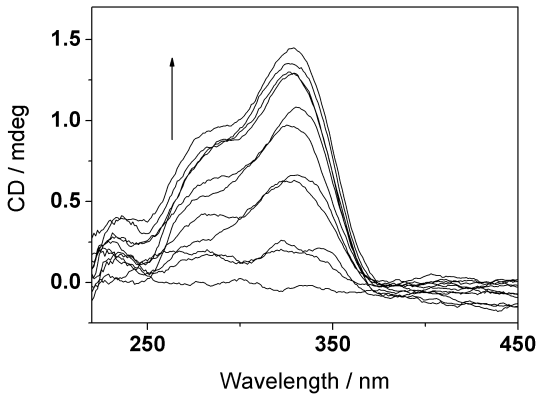

Figure S3. Polarimetric titration of HP-*β*-CD to **1** (c = 20 μM, $c_{\text{HP-β-CD}}/c_{\mathbf{1}}$ = 0–1000) in phosphate buffer (pH 7.0) at 20 °C.

NMR spectroscopy

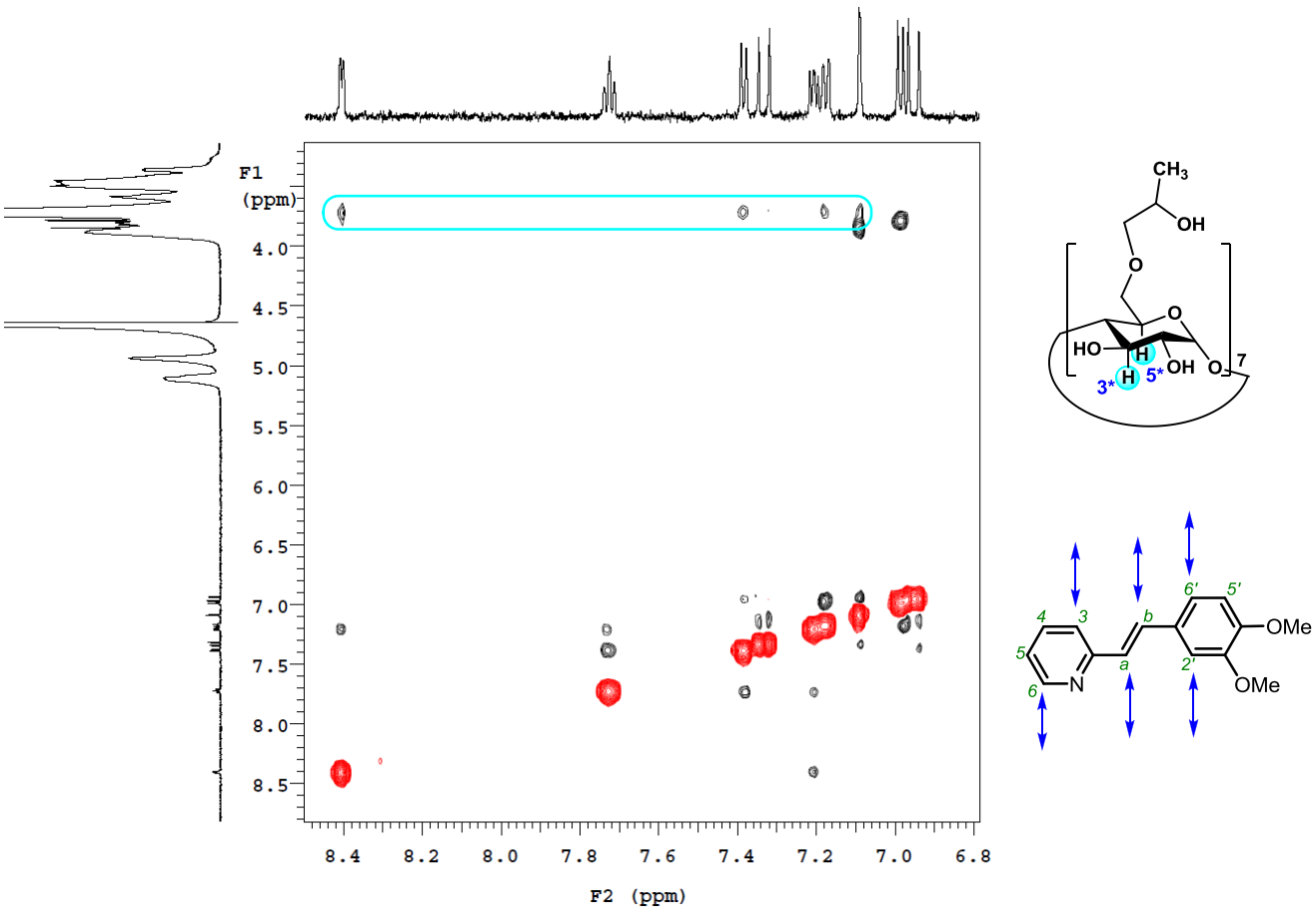

Figure S4. ROESY spectrum of styrylpyridine derivative **1** (c_1 = 0.3 mM) in the presence of a 10-fold excess of HP-β-CD in D_2O.

*3.2. Styrylpyridine derivative **1** – ct DNA interaction*

Absorption, fluorescence and circular dichroism spectroscopy

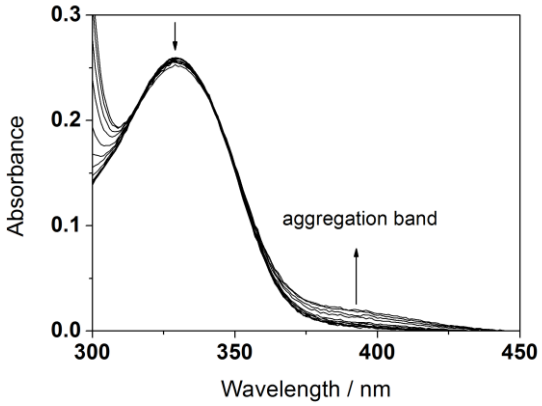

Figure S5. Spectrophotometric titration of ct DNA to **1** ($c_{\mathbf{1}}$ = 10 μM, $c_{DNA}/c_{\mathbf{1}}$ = 0–45) in phosphate buffer (pH 7.0) at 20 °C.

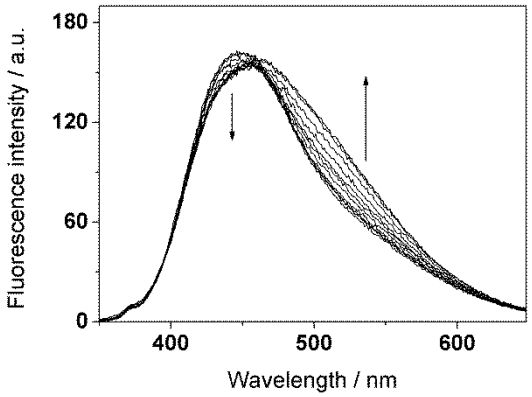

Figure S6. Fluorimetric titration of ct DNA to **1** (λ_{ex} = 330 nm, $c_{\mathbf{1}}$ = 10 μM, $c_{DNA}/c_{\mathbf{1}}$ = 0–52.6) in phosphate buffer (pH 7.0) at 20 °C.

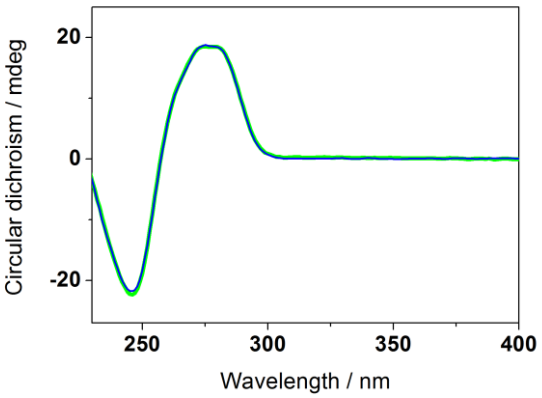

Figure S7. Circular dichroism spectra of ct DNA (green) and mixture of **1** and ct DNA (blue); c_{DNA} = 0.1 mM, $c_{\mathbf{1}}$ = 20 μM in phosphate buffer (pH 7.0) at 20 °C.

3.3. Styrylpyridine derivative 1 – CB[7] interaction

Absorption spectroscopy

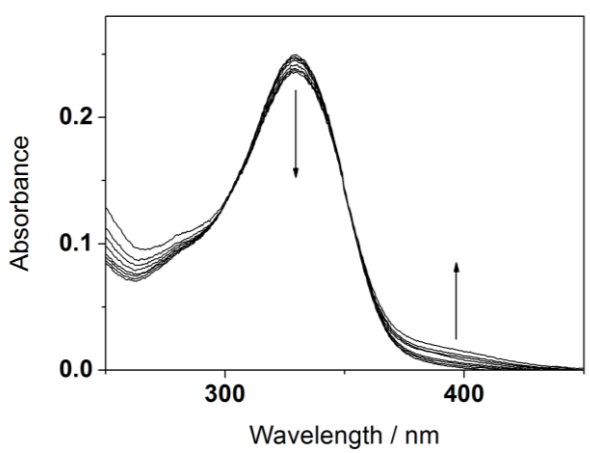

Figure S8. Spectrophotometric titration of CB[7] to **1** ($c_{\mathbf{1}}$ = 10 μM, $c_{CB[7]}$ /$c_{\mathbf{1}}$ = 0–30) in phosphate buffer (pH 7.0) at 20 °C.

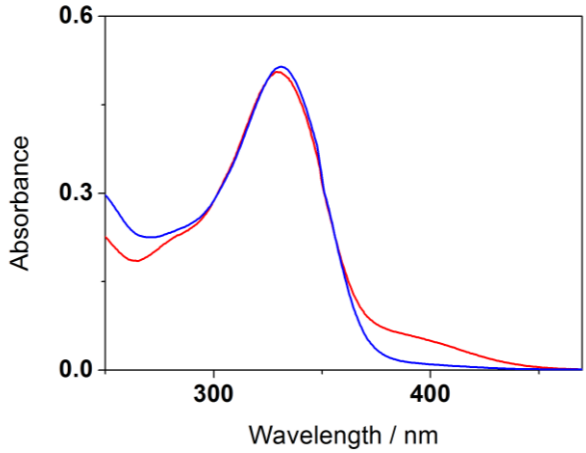

Figure S9. Suppression of the protonation of ligand **1** in the presence of CB[7] (red) upon addition of HP-*β*-CD (blue) in phosphate buffer (pH 7.0) at 20 °C ($c_{\mathbf{1}}$ = 20 μM, $c_{CB[7]}$ /$c_{\mathbf{1}}$ = 15, $c_{HP\text{-}\beta\text{-}CD}$ = 10 mM).

Protonation of the CB-bound ligand is a consequence of charge-dipole interactions between a cucurbituril host and a guest that result in the shifting of the pK_a of the guest towards higher values.[2] In contrast, the pK_a of a ligand decreases when bound to cyclodextrin because hydrophobic interactions are the dominant interactions in this complex.[3] Considering these differences the competition of the two hosts for ligand **1** at the applied pH value of 7.0 was assessed, *i. e.* when the non-protonated form of **1** prevails.

3.4. Photocyclization product **2** – HP-β-CD interaction

Circular dichroism spectroscopy

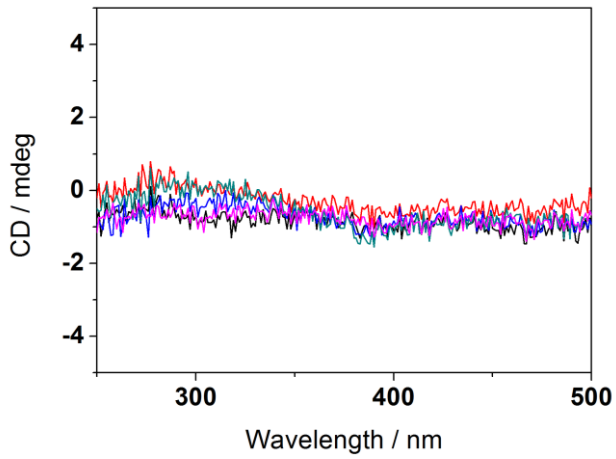

Figure S10. Circular dichroism spectra of ligand **2** ($c_{\mathbf{2}}$ = 20 μM) in the presence of HP-*β*-CD at HP-*β*-CD/ligand ratios: 0 (black); 250 (red); 500 (blue); 750 (green); 1000 (pink) in phosphate buffer (pH 7.0) at 20 °C.

*3.5. Photocyclization product **2** – ct DNA interaction*

Absorption, fluorescence and circular dichroism spectroscopy

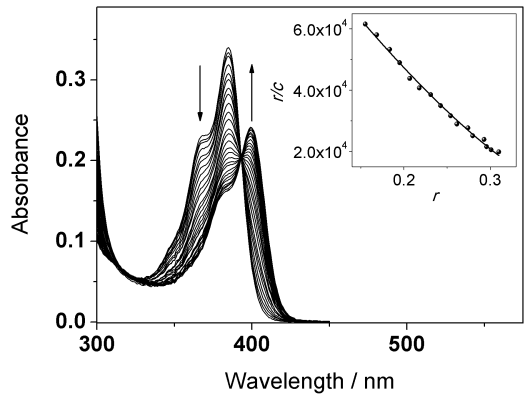

Figure S11. Spectrophotometric titration of ct DNA to ligand **2** (c_2 = 20 μM, c_{DNA} /c_2 = 0–17.2) in phosphate buffer (pH 7.0) at 20 °C. Inset: Scatchard plot *r/c vs. r*.

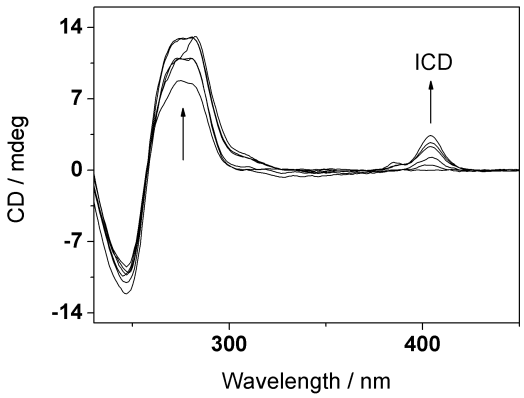

Figure S12. Circular dichroism spectra of mixtures of ct DNA (c_{DNA} = 50 μM, in base pairs) with ligand **2** at ligand-DNA ratio *LDR* = 0; 0.3; 0.5; 0.8; 1.0; in phosphate buffer (pH 7.0) at 20 °C.

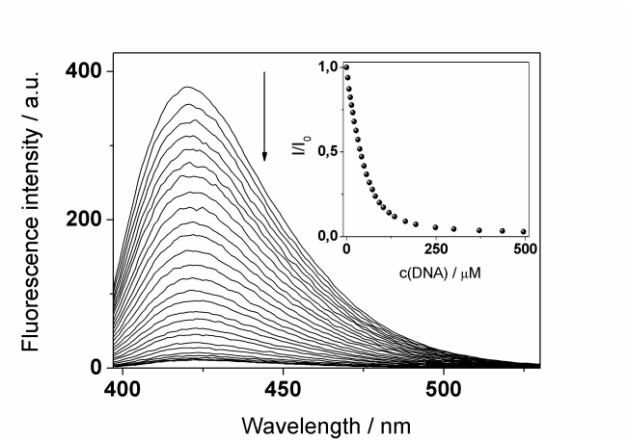

Figure S13. Fluorimetric titration of ct DNA to **2** (λ_{ex} = 393 nm, c_2 = 20 mM, c_{DNA}/ c_2 = 0–24.7) in phosphate buffer (pH 7.0) at 20 °C. Inset: plot of I/I_0 at 420 nm *vs.* c_{DNA}.

Thermal DNA denaturation

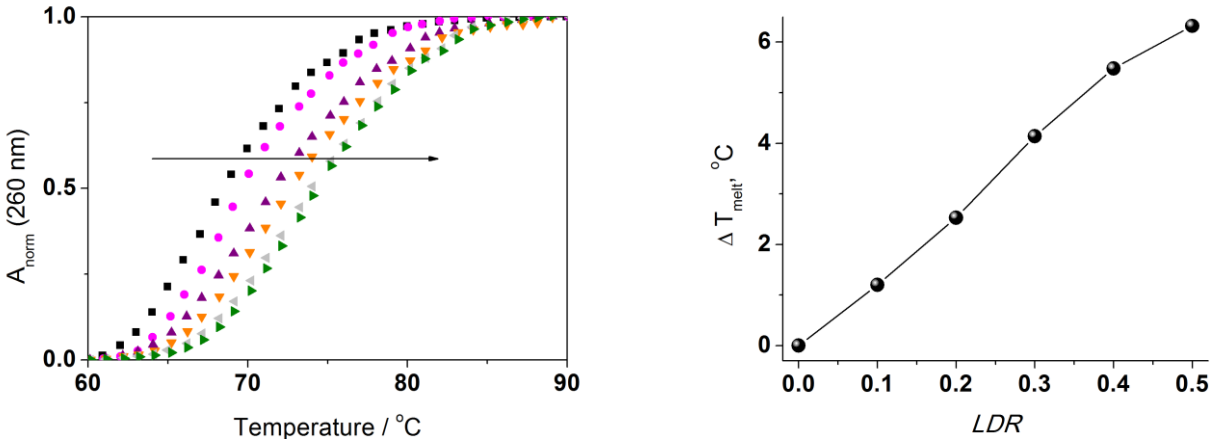

Figure S14. Normalized thermal denaturation curves of ct DNA in the presence of compound **2** at ligand-DNA ratios *LDR* = 0, 0.1, 0.2, 0.3, 0.4, 0.5; and a plot of induced T_m shifts versus *LDR*, c_{DNA} = 40 μM (base pairs) in phosphate buffer (pH 7.0).

Viscometry

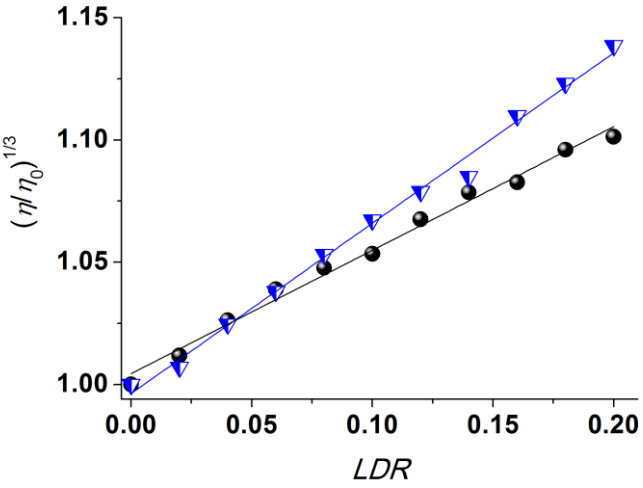

Figure S15. Relative specific viscosity of ct DNA in the presence of **2** (blue triangles) and ethidium bromide (black circles) as a function of the ligand-DNA ratio *LDR*, c_{DNA} = 1 mM (base pairs) in phosphate buffer (pH 7.0) at 20 °C.

*3.6. Photocyclization product **2** – CB[7] interaction*

Absorption spectroscopy

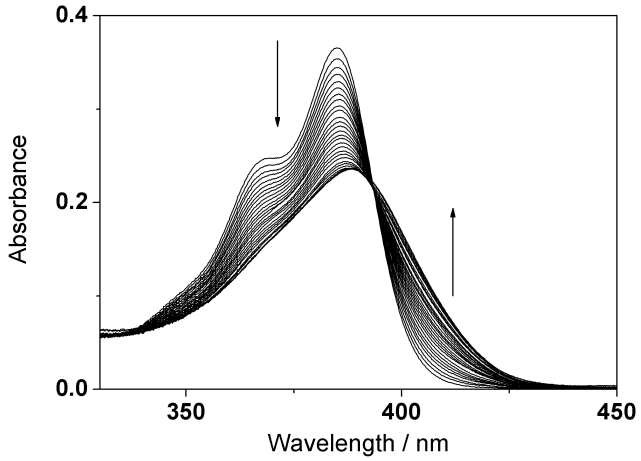

Figure S16. Spectrophotometric titration of CB[7] to **2** ($c_{\mathbf{2}}$ = 20 μM, $c_{CB[7]}/c_{\mathbf{2}}$ = 0–11.9) in phosphate buffer (pH 7.0) at 20 °C.

3.7. Interactions in the mixtures HP-β-CD – ct DNA – CB[7]

Circular dichroism spectroscopy

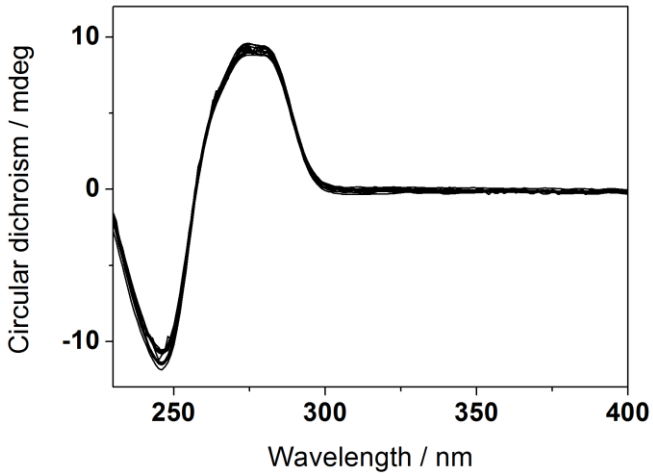

Figure S17. Circular dichroism spectra of ct DNA in the presence of HP-*β*-CD (c_{DNA} = 50 μM base pairs, $c_{HP\text{-}\beta\text{-}CD}/c_{DNA}$ = 0–1000) in phosphate buffer (pH 7.0) at 20 °C.

Thermal DNA denaturation

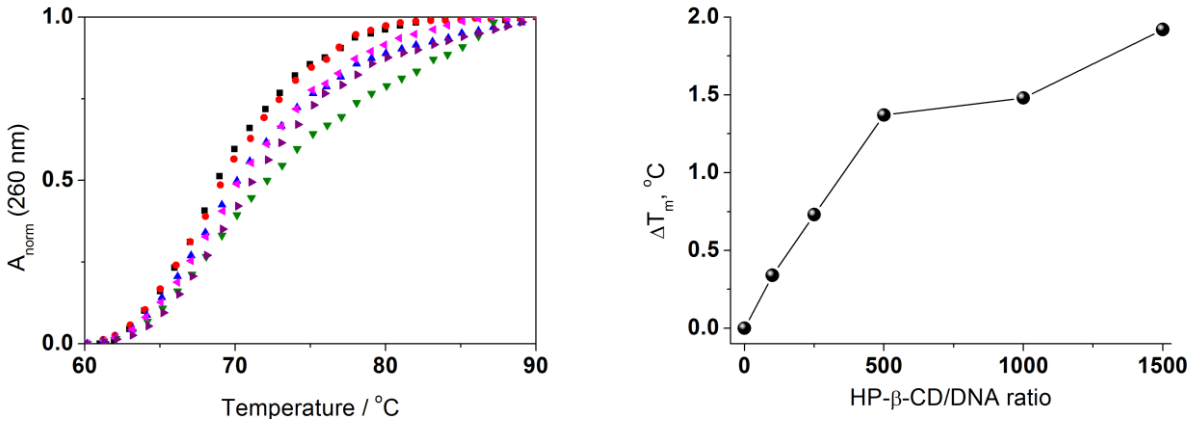

Figure S18. Normalized thermal denaturation curves of ct DNA in the presence of HP-*β*-CD at HP-*β*-CD–DNA ratios = 0, 100, 250, 500, 1000, 1500; and a plot of induced T_m shifts versus HP-*β*-CD-DNA ratio, c_{DNA} = 40 μM (base pairs) in phosphate buffer (pH 7.0).

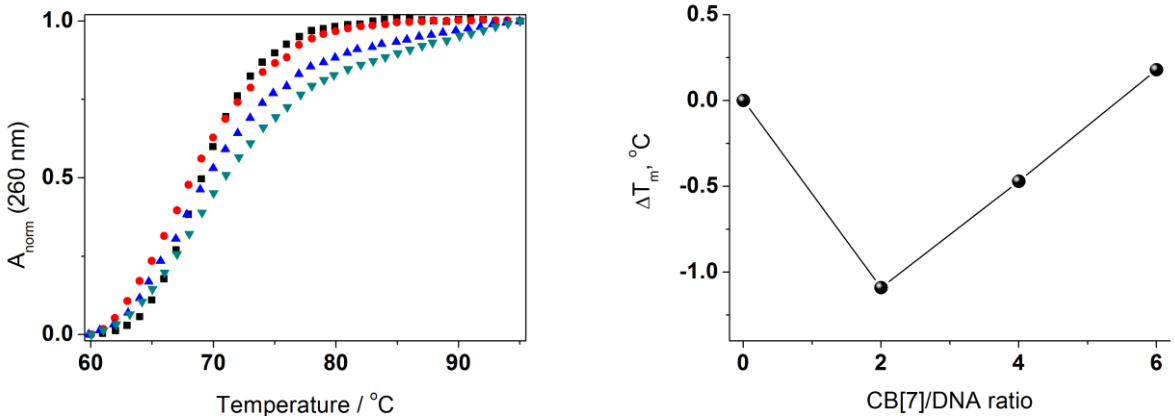

Figure S19. Normalized thermal denaturation curves of ct DNA upon addition of CB[7] at CB[7]-DNA ratios = 0, 2, 4, 6; and a plot of induced T_m shifts versus CB[7]-DNA ratio, c_{DNA} = 40 μM (base pairs) in phosphate buffer (pH 7.0).

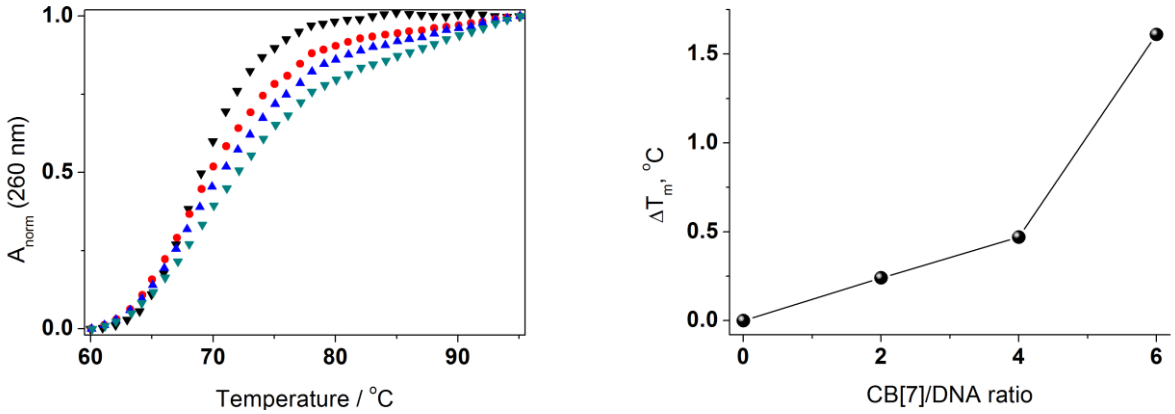

Figure S20. Normalized thermal denaturation curves of ct DNA upon addition of CB[7] and 500 molar eq. of HP-*β*-CD at CB[7]-DNA ratios = 0, 2, 4, 6; and a plot of induced T_m shifts versus CB[7]-DNA ratio, c_{DNA} = 40 μM (base pairs) in phosphate buffer (pH 7.0).

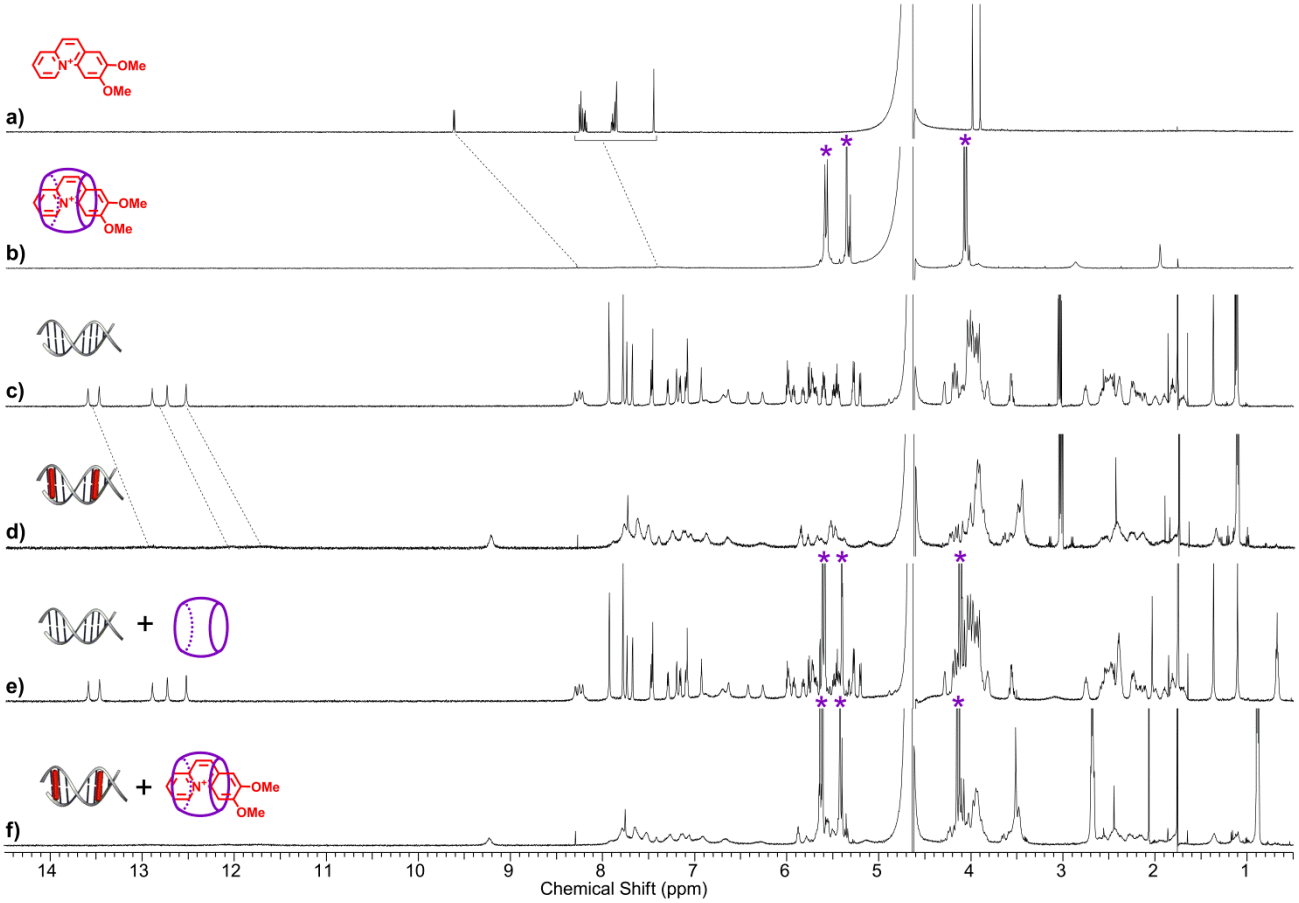

Figure S21. ^{1}H NMR spectra of (a): **2** (c_2 = 2 mM); (b): **2** in the presence of CB[7] (c_2 = 2 mM, $c_{CB[7]}$ = 2.6 mM); (c): Dickerson dodecamer 5'-CGCGAATTCGCG-3' (c_{DNA} = 2 mM); (d): Dickerson dodecamer in the presence of **2** (c_{DNA} = 2 mM, c_2 = 2 mM); (e): Dickerson dodecamer in the presence of CB[7] (c_{DNA} = 2 mM, $c_{CB[7]}$ = 2 mM); (f): Dickerson dodecamer in the presence of both **2** and CB[7] (c_{DNA} = 2 mM, $c_{CB[7]}$ = 2 mM, c_2 = 2 mM). In all cases: H_2O/D_2O (9:1) mixture containing phosphate buffer (10 mM, pH 7.0), NaN_3 (10μM), and EDTA (10μM); 25 °C. Signals of CB[7] are marked with an asterisk.

NMR data support the intercalative binding mode of compound **2**. Thus, upon addition of **2** (c_{DNA}/c_2 = 1) the signals of the imino protons of the DNA duplex (12.5–13.7 ppm) undergo a pronounced upfield shift along with significant broadening. Such a behavior indicates dynamic DNA intercalation that strongly affects the chemical environment of the DNA imino groups.[4]

4. Photochemical Studies

*4.1. Photocyclization of free styrylpyridine derivative **1***

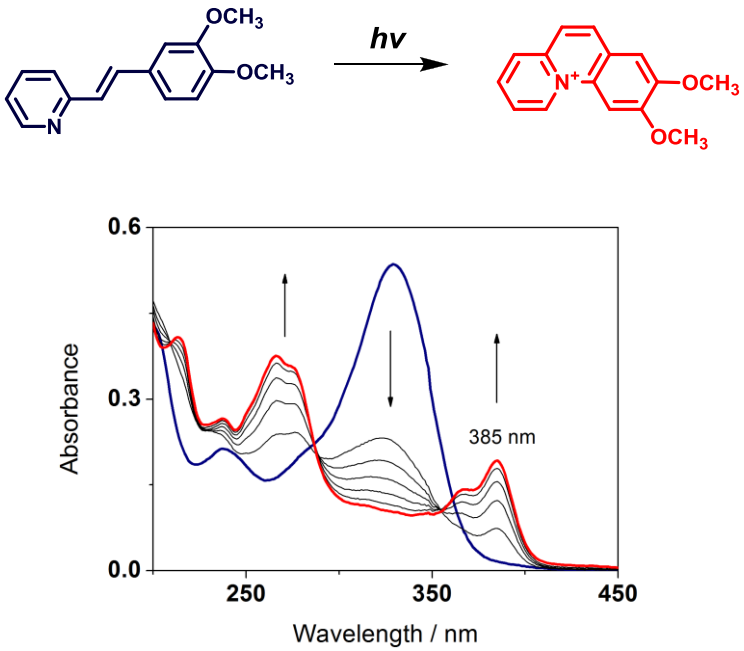

Figure S22. Photocyclization of **1** monitored by absorption spectroscopy ($c_{\mathbf{1}}$ = 20 μM, full light of a Hg lamp, spectra were recorded every 5 min, timescale 0–30 min) in phosphate buffer (pH 7.0) at 20 °C.

*4.2. Photocyclization of **1** encapsulated in the cavity of HP-β-CD*

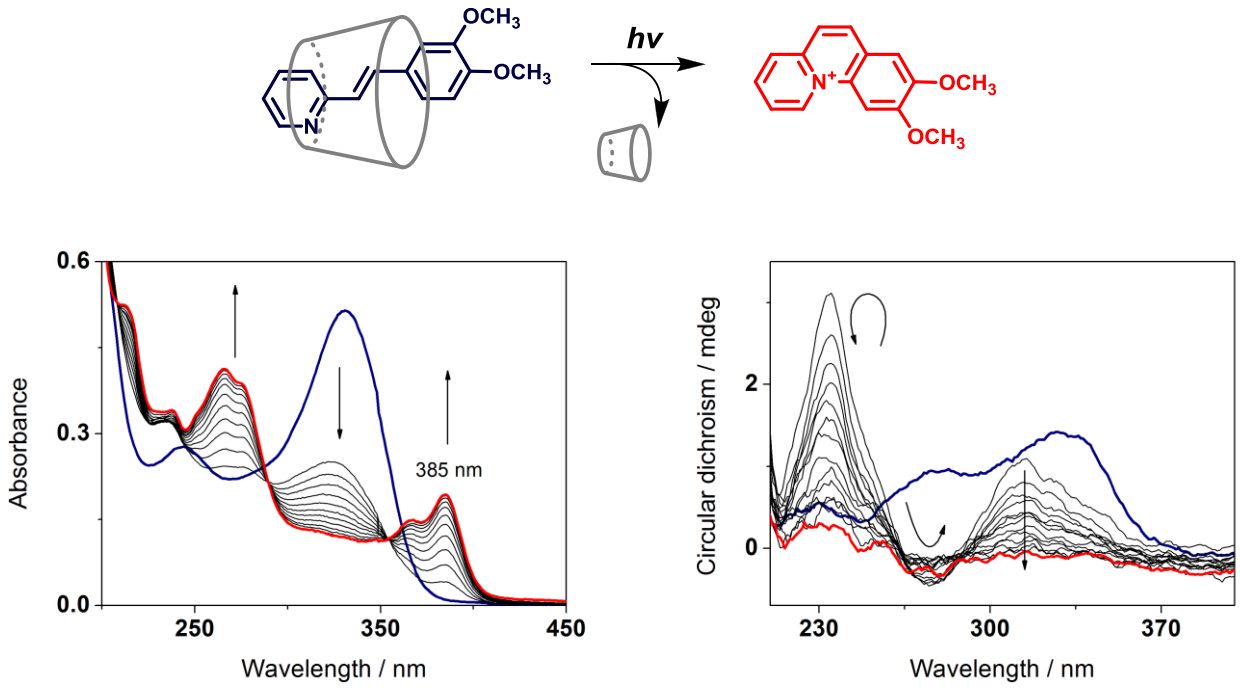

Figure S23. Photocyclization of **1** encapsulated in the cavity of HP-*β*-CD monitored by absorption (left) and CD (right) spectroscopy ($c_{\mathbf{1}}$ = 20 μM, $c_{\text{HP-}\beta\text{-CD}}$ = 10 mM, full light of a Hg lamp, spectra were recorded every 5 min, timescale 0–60 min) in phosphate buffer (pH 7.0) at 20 °C.

4.3. Photocyclization of **1** in the presence of ct DNA

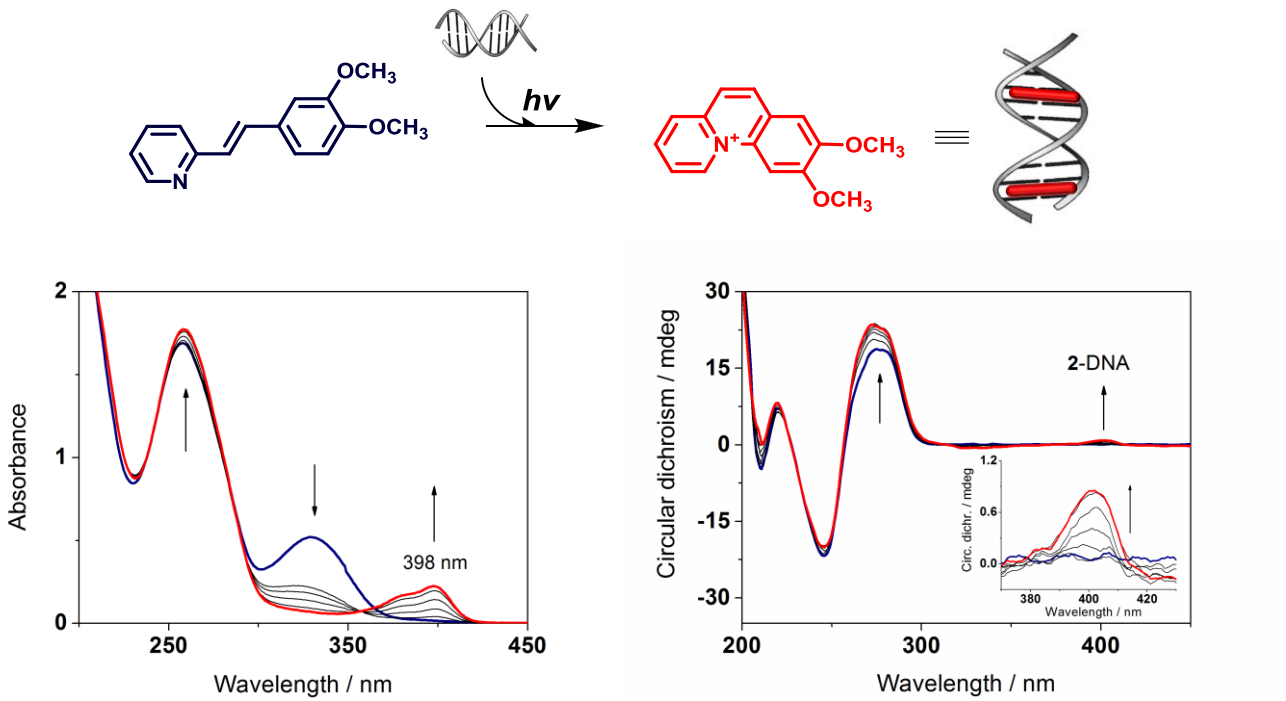

Figure S24. Photocyclization of **1** in the presence of ct DNA monitored by absorption (left) and CD (right) spectroscopy ($c_{\mathbf{1}}$ = 20 μM, c_{DNA} = 0.1 mM, full light of a Hg lamp, spectra were recorded every 5 min, timescale 0–30 min) in phosphate buffer (pH 7.0) at 20 °C.

4.4. Photocyclization of **1** encapsulated in HP-β-CD in the presence of CB[7] and ct DNA

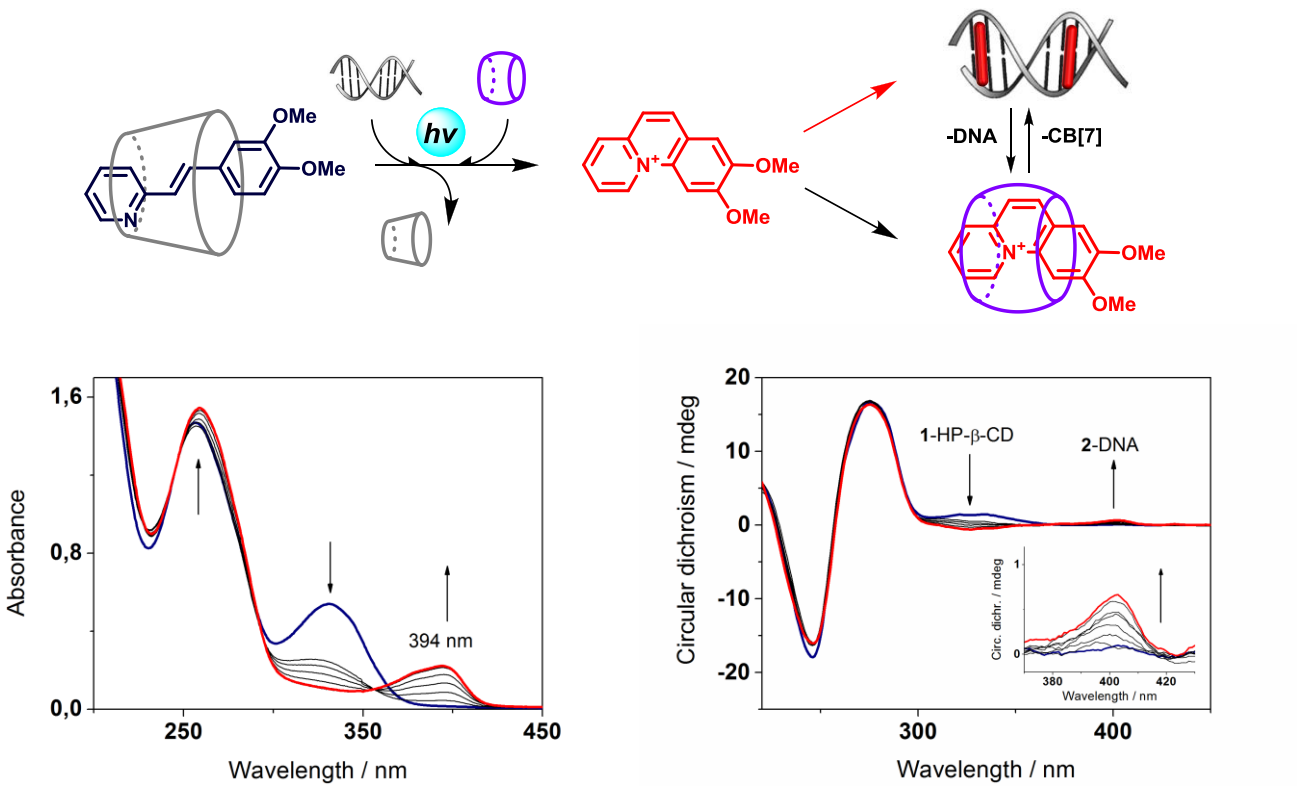

Figure S25. Photocyclization of **1** encapsulated in HP-β-CD in the presence of both ct DNA and CB[7] monitored by absorption (left) and CD (right) spectroscopy ($c_{\mathbf{1}}$ = 20 μM, $c_{HP\text{-}\beta\text{-}CD}$ = 10 mM, c_{DNA} = 0.1 mM, $c_{CB[7]}$ = 0.2 mM, full light of a Hg lamp, spectra were recorded every 5 min, timescale 0–30 min) in phosphate buffer (pH 7.0) at 20 °C.

5. Concurrent Binding of 2 with ct DNA and CB[7]

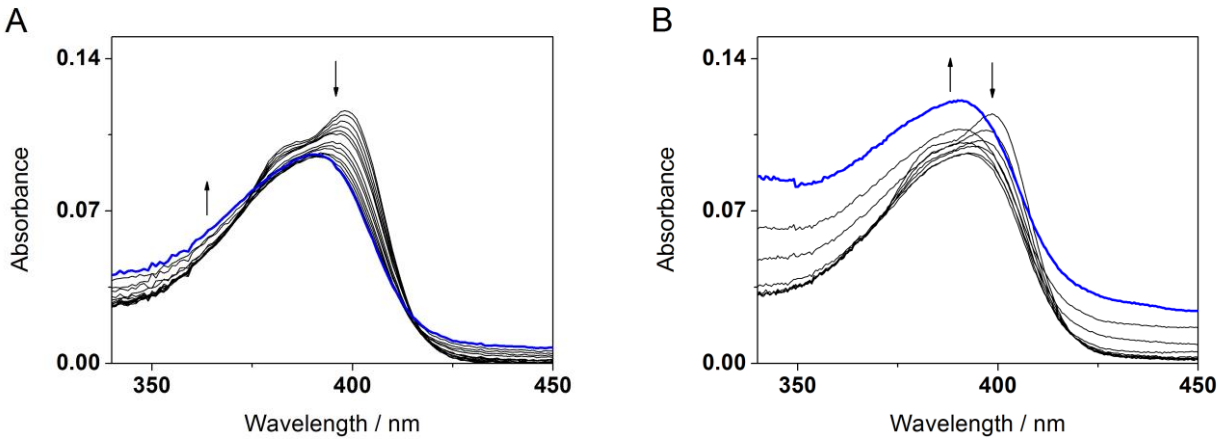

Figure S26. Absorption spectra of **2**–ct DNA mixtures upon addition of CB[7] in phosphate buffer ($c_{\mathbf{2}}$ = 10 μM, c_{DNA} = 80 μM: (a) without HP-β-CD, ($c_{CB[7]}$ /$c_{\mathbf{2}}$ = 0–42); (b) in the presence of 500 eq. of HP-β-CD ($c_{CB[7]}$ /$c_{\mathbf{2}}$ = 0–40, $c_{HP\text{-}\beta\text{-}CD}$ = 5 mM). Final spectra of the **2**-CB[7] complex are marked in blue.

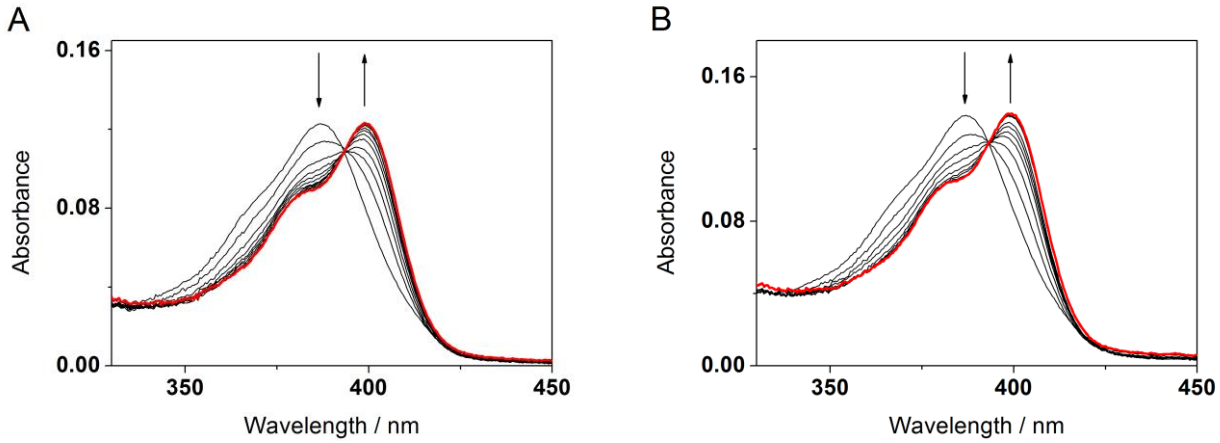

Figure S27. Absorption spectra of **2**–CB[7] mixtures upon addition of ct DNA in phosphate buffer ($c_{\mathbf{2}}$ = 10 μM, $c_{CB[7]}$ = 0.1 mM, c_{DNA} /$c_{\mathbf{2}}$ = 0–30): (a) without HP-β-CD; (b) in the presence of 500 eq. of HP-β-CD ($c_{HP\text{-}\beta\text{-}CD}$ = 5 mM). Final spectra of the **2**-DNA complex are marked in red.

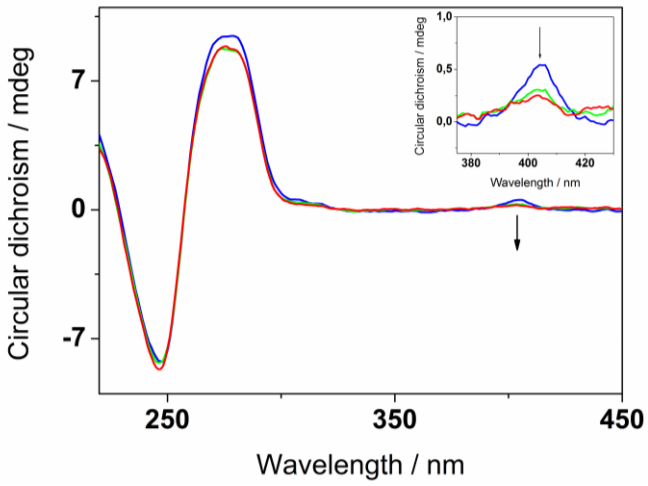

Figure S28. Circular dichroism spectra of **2**–ct DNA mixtures (c_2 = 15 μM, c_{DNA} = 50 μM) in phosphate buffer (pH 7.0) at 20 °C: blue: without CB[7]; green: in the presence of 5 eq. of CB[7] ($c_{CB[7]}$ = 75 μM); red: in the presence of 10 eq. of CB[7] ($c_{CB[7]}$ = 150 μM). Inset: Disappearance of the ICD signal of the **2**-DNA complex due to extraction of ligand **2** from the DNA helix by CB[7].

6. NMR Spectra

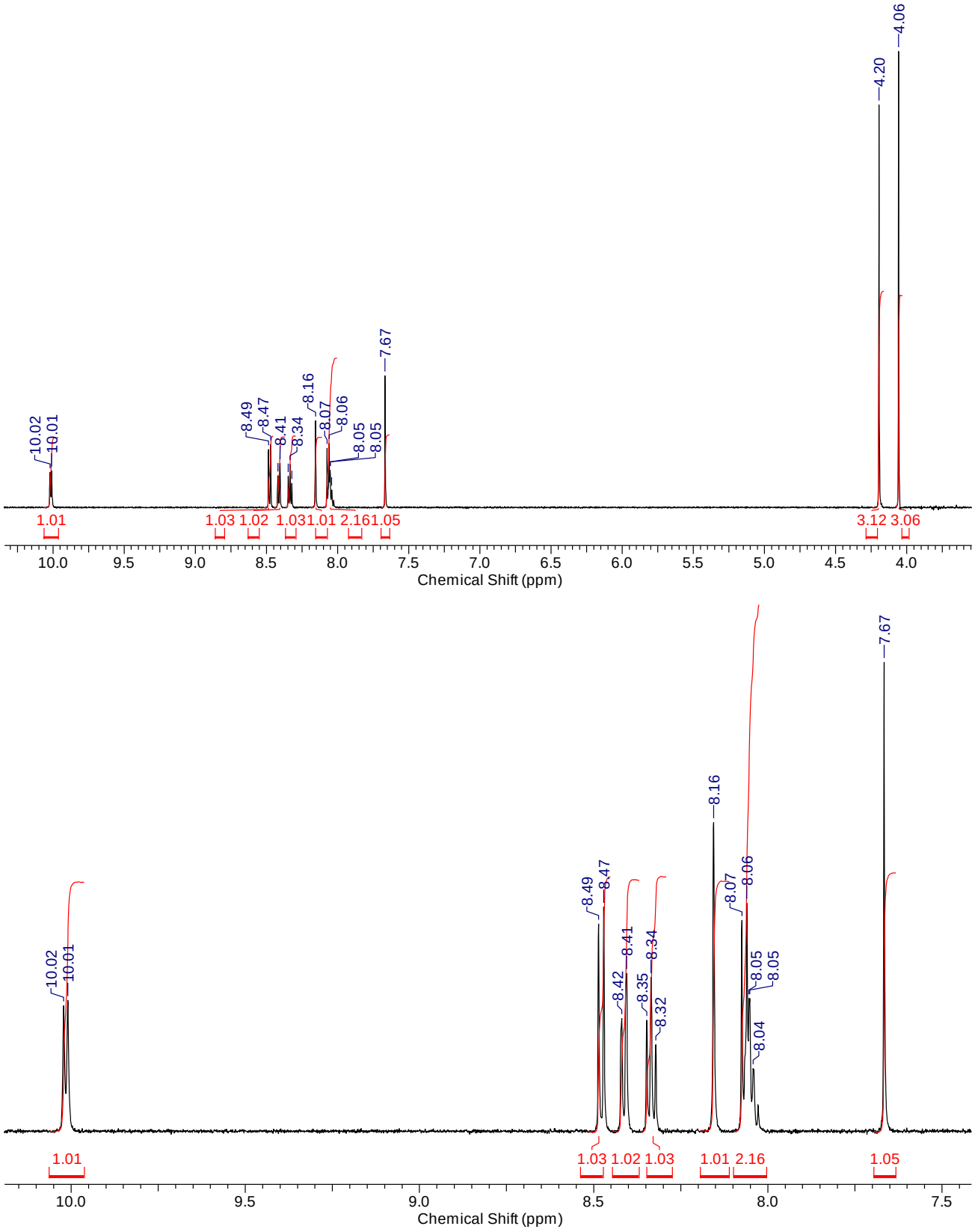

Figure S29. ^{1}H NMR spectrum of **2** in CD_3CN.

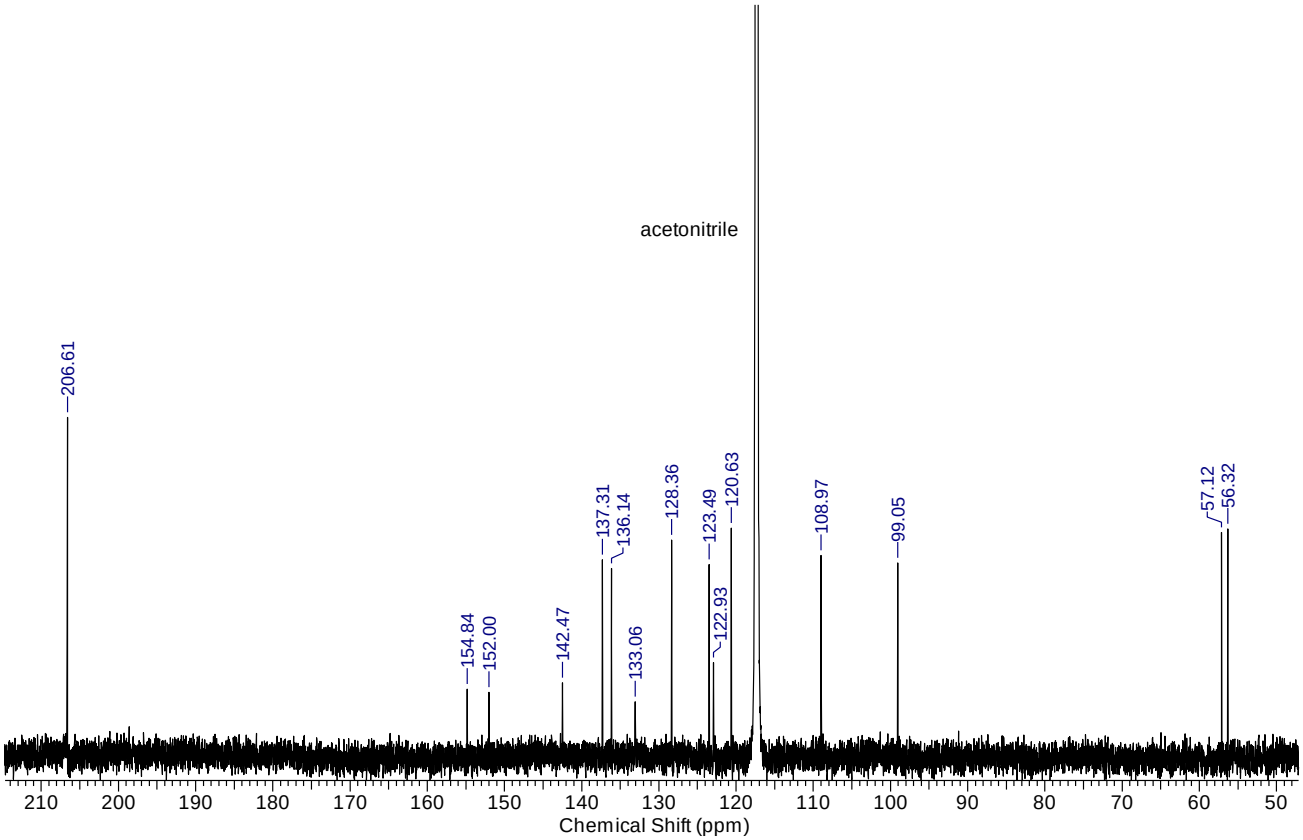

Figure S30. ^{13}C NMR spectrum of **2** in CD_3CN.

7. HRMS Data

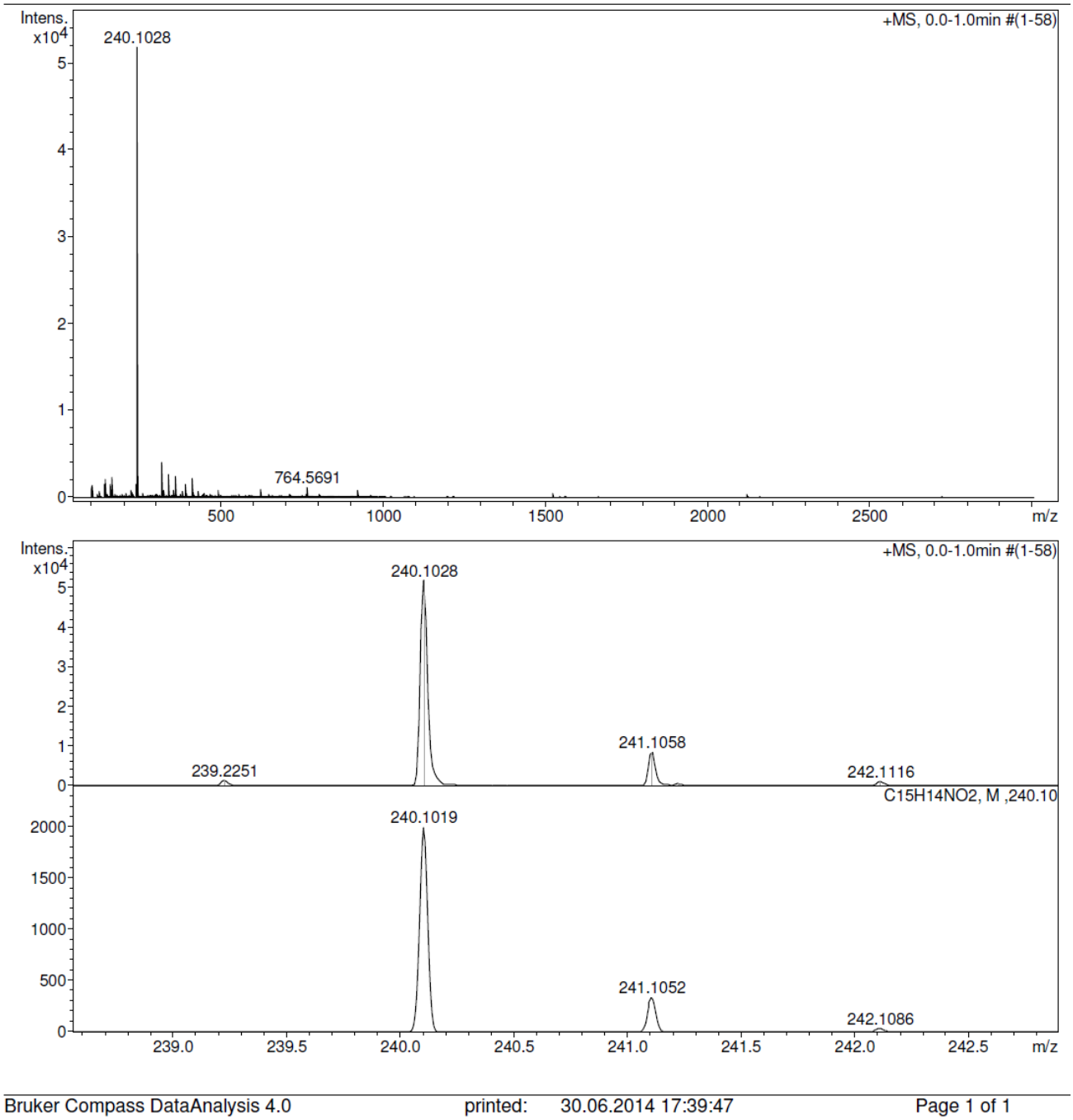

Figure S31. HRMS for **2** in CD_3CN; upper panels: experiment, lower panel: calculation.

References

1. C. Marquez, F. Huang, W. M. Nau, *NanoBioscience, IEEE Transact*. **2004**, *3*, 39.
2. N. Barooah, J. Mohanty, H. Pal, A. C. Bhasikuttan, *Proc. Natl. Acad. Sci., India, Sect. A Phys. Sci*., 2014, **84**, 1.
3. M. Shaikh, J. Mohanty, P. K. Singh, W. M. Nau, H. Pal, *Photochem. Photobiol. Sci*., **2008**, *7*, 408.
4. (*a*) J. Feigon, W. A. Denny, W. Leupin and D. R. Kearns, *J. Med. Chem.*, 1984, **27**, 450; (*b*) M. A. Keniry and R. H. Shafer, *Methods Enzymol.*, 1995, **261**, 575; (*c*) L. Strekowski and B. Wilson, *Mutat. Res.*, 2007, **623**, 3.